Conservative and Nonconservative Mutations of the Transmembrane CPC Motif in ZntA: Effect on Metal Selectivity and Activity†

Sabari J. Dutta, Junbo Liu, Ann J. Stemmler, and Bharati Mitra*

Department of Biochemistry and Molecular Biology, School of Medicine, Wayne State University, Detroit, Michigan 48201

Received August 11, 2006; Revised Manuscript Received January 22, 2007

ABSTRACT: ZntA from *Escherichia coli* belongs to the P_{1B}-ATPase transporter family and mediates resistance to toxic levels of selected divalent metal ions. P_{1B}-type ATPases can be divided into subgroups based on substrate cation selectivity. ZntA has the highest selectivity for Pb^{2+}, followed by Zn^{2+} and Cd^{2+}; it also shows low levels of activity with Cu^{2+}, Ni^{2+}, and Co^{2+}. It has two high-affinity metal-binding sites, one each in the N-terminus and the transmembrane domains. Ligands to the transmembrane metal site in ZntA include the cysteine residues of the conserved ^{392}CPC^{394} motif in the sixth transmembrane helix. Pro393 is invariant in all P-type ATPases. For ZntA homologues with different metal ion selectivity, the cysteines are replaced by serine, histidine, and threonine. To test the effect on activity and metal ion selectivity, single alanine, histidine, and serine substitutions at Cys392 or Cys394 in ZntA were characterized, as well as double substitutions of both cysteines by histidine or serine. P393A was also characterized. C392A, C394A, and P393A lost the ability to bind a metal ion with high affinity in the transmembrane domain. Histidine and serine substitutions at Cys392 and Cys394 resulted in loss of binding of Pb^{2+} at the transmembrane site, indicating that both cysteines of the CPC motif are required for binding Pb^{2+} with high affinity in ZntA homologues. However, C392H, C392S, C394H, C394S, C392S/C394S, and C392H/C394H could bind other divalent metal ions at the transmembrane site and retained low but measurable activity. Interestingly, these mutants lost the predominant selectivity for Zn^{2+} and Cd^{2+} shown by wtZntA. Therefore, conserved residues contribute to metal selectivity by supplying ligands that bind metal ions not only with high affinity, as for Pb^{2+}, but also with the most favorable binding geometry that results in efficient catalysis.

ZntA from *Escherichia coli* is a member of the P-type ATPase cation transporter superfamily (*1*). These pumps form an acylphosphate intermediate following ATP hydrolysis during the catalytic cycle together with cation translocation across membranes. They have been divided into phylogenetically distinct groups (*2*). One of these, P_{1B}-type ATPases, found in archaea, bacteria, and eukarya, including humans, transports soft metal ions such as Pb^{2+}, Zn^{2+}, Cd^{2+}, Co^{2+}, Cu^{2+}, Cu^{+}, and Ag^{+} (*2*−*14*). The P_{1B}-type pumps are important for maintaining homeostasis of essential soft metals such as cobalt, copper, and zinc in organisms. They also confer resistance to toxic metals such as cadmium, lead, and silver in bacteria and plants. In vivo, ZntA confers resistance to toxic concentrations of divalent cations, such as Pb^{2+}, Zn^{2+}, and Cd^{2+}, by active efflux of these metal ions outside the cytoplasm (*8*, *9*).

P_{1B}-type ATPases contain three domains. The first is a hydrophilic N-terminal segment containing one to six metal-binding sites (*2*, *15*−*19*). A second domain contains the large hydrophilic segments that are the sites for ATP binding and hydrolysis and the acylphosphate intermediate formation and breakdown (*1*, *2*). The third domain is membrane-bound and has eight membrane-spanning helices; our earlier work on ZntA has shown that this domain has a single high-affinity metal-ion-binding site (*20*). P_{1B}-type ATPases can be further subdivided into different subgroups based on sequence alignment and putative metal selectivity (*21*); these are selective for Zn^{2+}/Pb^{2+}/Cd^{2+}, Cu^{+}/Ag^{+}, Cu^{2+}, Co^{2+}, and as yet unassigned metal ions. The molecular basis of metal ion selectivity in P_{1B}-type pumps is not yet clearly understood, though insights are emerging from biochemical and structural studies (*19*, *20*, *22*, *23*).

The metal-binding site in the N-terminal domain for pumps selective for transporting Cu^{+} and Ag^{+} or Zn^{2+}, Pb^{2+}, and Cd^{2+} has the cysteine-containing motif GXXCXXC (*3*, *7*, *8*, *11*−*13*). Pumps selective for Zn^{2+} and Cd^{2+} have, in addition, a conserved acidic residue, an aspartic acid or a glutamic acid, that has been shown to be a metal-binding ligand in structural studies (*22*, *23*). Zn^{2+} and Cd^{2+} are bound at the N-terminal site in tetrahedral coordination to two cysteine residues and the carboxylate oxygens of the aspartic/glutamic acid residue. ZntA from *E. coli* shows the highest selectivity for Pb^{2+} (*24*). ZntA and close homologues, including those from *Salmonella typhi* and *Klebsiella pneumoniae*, contain an additional cysteine-rich motif, CCX(D,E)-

† This work was supported by United States Public Health Service Grant GM-61689 (to B.M.). S.J.D. was supported by an American Heart Association postdoctoral fellowship.

* To whom correspondence should be addressed. Mailing address: Department of Biochemistry and Molecular Biology, Wayne State University School of Medicine, 540 E. Canfield Avenue, Detroit, Michigan 48201. E-mail: bmitra@med.wayne.edu. Phone: (313) 577-0040. Fax: (313) 577-2765.

10.1021/bi0616394 CCC: $37.00 © 2007 American Chemical Society
Published on Web 02/28/2007

XXC, in the N-terminal domain. One or more cysteines from this motif is required for binding Pb^{2+} but not Cd^{2+} or Zn^{2+} at the N-terminal site in ZntA; this motif is thus present in pumps that are highly selective for Pb^{2+} (*19*). The N-terminal site in Cu^{2+}-selective pumps is a histidine-rich motif, (M,H)-XXMDH(S,G)XM (*7*, *14*). A different histidine-rich motif, $(HX)_n$, is present in a few homologues of unknown function. Putative Co^{2+}-selective pumps do not have a metal-ion-binding N-terminal domain (*10*). ZntA, which is highly selective for Pb^{2+}, Cd^{2+}, and Zn^{2+}, is able to bind Cu^{2+}, Ni^{2+}, and Co^{2+}, in addition to Pb^{2+}, Cd^{2+}, and Zn^{2+}, with similar affinity at the N-terminal site (*19*). These observations suggest that metal selectivity at the N-terminal site is achieved by specific conserved residues that regulate metal binding geometry as well as affinity.

No structural studies have been reported yet for the metal-binding site in the transmembrane domain. While the N-terminal metal binding site is important for the physiological role of these pumps, it is not essential for activity. Mutant versions of the pumps in which the N-terminal site is knocked out or completely deleted show somewhat decreased activity but the same metal selectivity as the wild-type versions. Unlike the N-terminal site, the transmembrane site is essential for activity of the pump (*20*). The different subgroups of P_{1B}-ATPases have distinct patterns of conserved polar residues in the transmembrane segments; these may be the primary ligands for the transmembrane metal site or residues present in the secondary shell. Transmembrane helix six in all P_{1B}-type ATPases contains the conserved residues, (C,S,T)P(C,H) (Figure 1). The motif is strictly conserved as CPC for pumps that are selective for transporting Cu^+; Ag^+; or Zn^{2+}, Pb^{2+}, and Cd^{2+}. In pumps selective for Co^{2+} and Cu^{2+}, the conserved motifs are SPC and CPH, respectively. A subgroup of P_{1B}-type ATPases with unknown cation selectivity has a TPC motif (*21*). The cysteine residues flanking the invariant proline are necessary for overall activity. In Cu^+-ATPases from *E. coli* and *Archaeoglobus fulgidus*, site-specific mutagenesis of the two cysteines resulted in complete loss of overall activity (*25*, *26*). A similar result was obtained when the cysteines in a Cd^{2+}-ATPase from *Listeria monocytogenes*, CadA, were modified by the thiol-reactive reagent, *N*-ethylmaleimide (*27*). A recent study reported that while the C354A mutant of the *L. monocytogenes* CadA had no ATPase activity, the C356A mutant showed decreased levels of ATPase activity, though neither mutant showed *in vivo* activity (*28*). In ZntA, the C392A/C394A double mutant lost the ability to bind metal ions and was completely inactive (*20*). Thus, either or both cysteine residues in TM6 in these subgroups provide ligands to the metal ion in the transmembrane cation-binding site; this metal binding site is essential for the function of the pump.

In this study, the importance of each individual cysteine residue in metal ion binding was evaluated. More importantly, the effect of altering the individual cysteines to serine and histidine as observed in the Co^{2+} and Cu^{2+} pumps, respectively, on metal selectivity in ZntA was examined. Individual alanine substitutions at both Cys392 and Cys394 had no activity and lost the ability to bind a metal ion at the transmembrane site. The serine and histidine mutants were able to bind Zn^{2+}, Cd^{2+}, Ni^{2+}, Co^{2+}, and Cu^{2+} with affinity similar to wtZntA and had both in vivo and in vitro activity,

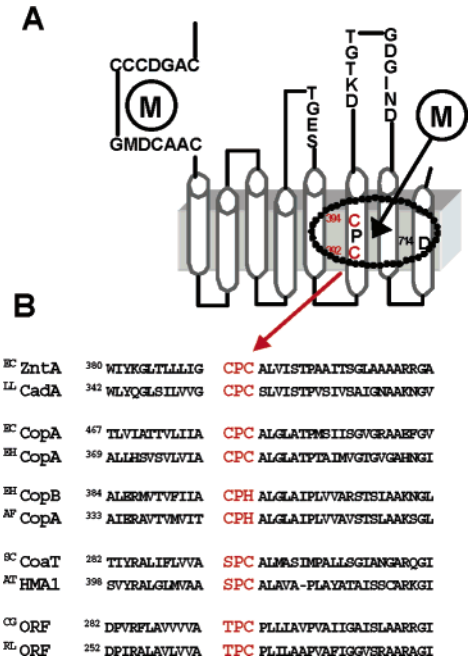

FIGURE 1: Panel A provides a schematic representation of ZntA showing the location of the two metal binding sites, in the N-terminal and the transmembrane domains. The cylinders represent the eight transmembrane domains. The positions of the CPC motif and Asp714 are indicated. Panel B presents a sequence alignment of TM6 in different subgroups of P_{1B}-ATPases, showing the variations in the CPC motif. ^{EC}ZntA, ZntA from *E. coli*, and ^{LL}-CadA, CadA from *Lactococcus lactis*, represent pumps selective for Zn^{2+}, Cd^{2+}, and Pb^{2+}; ^{EC}CopA, CopA from *E. coli*, and ^{EH}-CopA, CopA from *Enterococcus hirae*, represent pumps selective for Cu^+ and Ag^+; ^{EH}CopB, CopB from *E. hirae*, and ^{AF}CopA, CopA from *A. fulgidus*, represent pumps selective for Cu^{2+}; ^{SC}CoaT, CoaT from *Synechocystis* PCC6803, and ^{AT}HMA1, an ATPase from *Arabidopsis thaliana*, represent pumps believed to be selective for Co^{2+}; ^{CG}ORF and ^{RL}ORF, putative ATPases from *Corynebacterium glutamicum* (accession number, NP599727) and *Mesorhizobium loti* (accession number, NP107067), respectively, belong to a distinct subgroup of P_{1B}-type ATPases with unknown cation selectivity.

but the activity with these metal ions was much lower compared with wtZntA. Double serine and histidine mutants showed lower levels of activity than the individual mutants. The behavior of Pb^{2+} was surprisingly different; the serine and histidine mutants lost the ability to bind Pb^{2+}, indicating that both cysteines of the CPC motif are essential for binding Pb^{2+}. Substitution of the invariant Pro393 with alanine resulted in no overall activity with any metal and the inability to bind metal at the transmembrane site. These results support the hypothesis that conserved residues in the transmembrane site in P_{1B}-type ATPases contribute to metal selectivity by affecting optimal metal-binding geometry and in turn ATP hydrolysis and metal transport for most of the transported cations. For Pb^{2+}, selectivity is achieved by conserving residues that selectively bind this cation.

EXPERIMENTAL PROCEDURES

Construction of the C392A, C392S, C392H, C394A, C394S, C394H, C392H/C394H, C392S/C394S, and P393A Mutants. All the mutants were generated using the Quick-change Site-Directed Mutagenesis kit (Stratagene). The following oligonucleotides (from Integrated DNA Technologies, Coralville, IA) were used:

C392A, 5′-CTG CTG CTG ATT GGC **GC**C CCG TGT GCG TTA G-3′ and 5′-C TAA CGC ACA CGG G**GC** GCC AAT CAG CAG CAG-3′

C392S, 5′-CTG ATT GGC T**C**C CCG TGT GCG TTA GTG ATA TCA ACG CC-3′ and 5′-GG CGT TGA TAT CAC TAA CGC ACA CGG G**G**A GCC AAT CAG-3′

C392H, 5′-CTG ATT GGC **CA**C CCG TGT GCG TTA GTG ATA TCA ACG CCT G-3′ and 5′-C AGG CGT TGA TAT CAC TAA CGC ACA CGG G**TG** GCC AAT CAG-3′

C394A, 5′-G ATT GGC TGC CCG **GC**T GCG TTA GTG ATA TCA ACG CCT G-3′ and 5′-C AGG CGT TGA TAT CAC TAA CGC A**GC** CGG GCA GCC AAT C-3′

C394S, 5′-G ATT GGC TGC CCG T**C**T GCG TTA GTG ATA TCA ACG CC-3′ and 5′-GG CGT TGA TAT CAC TAA CGC A**G**A CGG GCA GCC AAT C-3′

C394H, 5′-CTG CTG ATT GGC TGC CCG **CA**T GCG TTA GTT ATC TC-3′ and 5′-GA GAT AAC TAA CGC A**TG** CGG GCA GCC AAT CAG CAG-3′

P393A, 5′-CTG ATT GGC TGC **G**CG TGT GCG TTA GTG ATA TCA ACG CCT G-3′ and 5′-C AGG CGT TGA TAT CAC TAA CGC ACA CG**C** GCA GCC AAT CAG-3′

The altered bases for the desired mutations are indicated in boldface. In some cases, silent base changes (underlined) were used to create an *Eco*RV restriction site for rapid identification of the desired mutations. The sequences of the mutant genes were verified by automated DNA sequencing (Wayne State University). They were cloned in the pBAD/*Myc*-His C or pBAD/*Myc*-His A vector (Invitrogen) and expressed in strain LMG194(*zntA*::*cat*) as previously described for ZntA; in the first vector, the proteins are expressed with a carboxyl terminal histidyl tag, while in the latter vector, the proteins are expressed without any affinity tag (*20*, *24*).

Sensitivity to Soft Metal Salts. Strain LMG194(*zntA*::*cat*) in which the entire *zntA* gene is deleted is highly sensitive to the presence of metal salts in the growth medium; this sensitivity can be complemented by plasmids carrying the *wtzntA* gene (*19*). The sensitivity of LMG194, as well as LMG194(*zntA*::*cat*) transformed with plasmids containing recombinant, His-tagged *wtzntA* and the individual mutants at Cys392 and Cys394 to metal salts was measured as described earlier (*19*). Cells were grown in a basal salts medium containing lead acetate, zinc chloride, or cadmium chloride at different concentrations. Cell growth at 37 °C was measured by monitoring the absorbance at 600 nm.

Purification of Non-His-Tagged Proteins for Metal Binding Studies. Proteins were purified without any affinity tag. Proteins without an affinity tag were expressed in strain LMG194(*zntA*::*cat*) and purified using a Talon-affinity column (BD Biosciences Clontech) as described earlier; this method takes advantage of the intrinsic metal affinity of the proteins as long as at least one high-affinity site is intact (*20*, *29*). Purity of the proteins and the absence of the His tag were confirmed by SDS-PAGE[1] and Western blotting using anti-His antibody (Invitrogen).

Free Thiol Quantitation. The number of free thiols in native and denatured, metal-free proteins was quantified using a standard DTNB assay as described before to ensure that proteins stayed reduced for the duration of the metal-binding experiment (*19*, *30*).

Measurement of Metal-Binding Stoichiometry and Affinity of the Cys392 and Cys394 Mutants. Buffers and water used in these experiments were deoxygenated by flushing with argon and passed through Chelex 100 (Sigma) to remove extraneous metal salts. Metal-binding stoichiometry was measured using ICP-MS as described before (*19*). Reduced apoprotein was prepared by treating purified proteins with 2 mM DTT and 5 mM EDTA at 4 °C for 1 h, followed by removal of DTT and EDTA by passage over two consecutive Sephadex G-25 columns equilibrated in 10 mM Bis−Tris, pH 7.0, containing 0.5 mM DDM, under anaerobic conditions. For stoichiometry measurements, the apoprotein was incubated with different metal salt solutions for 1 h at 4 °C in 10 mM Bis-Tris, pH 7.0, containing 0.5 mM DDM, followed by removal of excess metal ions using Sephadex G-25 columns. Samples were digested with concentrated nitric acid and diluted, and metal content was determined by ICP-MS (metal standards for ICP-MS were from VWR).

The affinity for Pb^{2+}, Zn^{2+}, and Cd^{2+} was determined at 20 °C by competition titration with the metal indicator mag-fura-2 (Molecular Probes) in 10 mM BisTris, pH 7.0, and 0.5 mM DDM as described previously (*19*, *20*). Mag-fura-2 forms a 1:1 complex with divalent metal ions; the metal-free form has an absorbance maximum at 366 nm, which changes to ∼325 nm when metal is bound. The decrease in absorbance at 366 nm as increasing amounts of metal ion was bound to the indicator in competition with the protein was recorded. Titration was performed with reduced, anaerobic proteins.

The affinity of wtZntA and the mutant proteins for different metal ions (Pb^{2+}, Zn^{2+}, Cd^{2+}, Cu^{2+}, Co^{2+}, and Ni^{2+}) was also determined by fluorescence titration of the reduced apoproteins with metal salt solutions in a Perkin-Elmer LS55 spectrofluorimeter. In this experiment, EDTA was used as a competitor of the proteins for the metal ions. Aliquots of metal salt solutions were added to a mixture of reduced apoprotein and ∼5 μM EDTA in 10 mM Bis-Tris, pH 7.0, and 0.5 mM DDM at 20 °C. Following each addition, the solution was mixed well, and the reduction in the intrinsic tryptophan fluorescence emission spectrum was recorded (excitation wavelength, 290 nm). The dilution following each addition of metal salt solution was taken into account when fitting the data.

ATPase and Acylphosphate Activity Assays. The metal-ion-dependent ATPase activity reported here was determined using a coupled assay with pyruvate kinase and lactate dehydrogenase as described earlier but with the following modification (*24*). Purified non-His-tagged proteins were thawed and incubated with 2 mM dithiothreitol (DTT) at 4 °C for 1 h, followed by removal of the DTT using Sephadex G-25 column chromatography. The reduced proteins were used within 30−60 min for activity measurements. Assays were at pH 7 and 37 °C. In some assays, the thiolate form of cysteine was added to the assay buffer at a concentration equal to that of the metal ion (1 M cysteine at pH 7.0 is equivalent to 44.7 mM of the thiolate form of cysteine).

[1] Abbreviations: Bis-Tris, bis(2-hydroxyethyl)amino-tris(hydroxymethyl)methane; ΔN-ZntA: a mutant of ZntA with residues 2−106 deleted; DDM, *n*-dodecyl-β-D-maltoside; DTNB, 5,5′-dithiobis(2-nitrobenzoic acid); EDTA, ethylenediaminetetraacetic acid; EXAFS, extended X-ray absorption fine structure; ICP-MS, inductively coupled plasma mass spectrometry; SDS-PAGE, sodium dodecyl sulfate polyacrylamide gel electrophoresis.

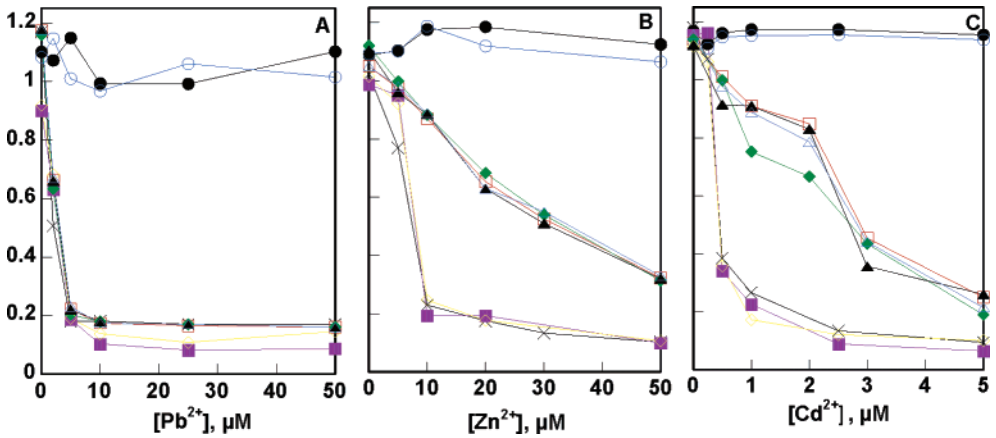

FIGURE 2: Resistance to Pb^{2+}, Zn^{2+}, and Cd^{2+} salts by the wild-type strain LMG194 (●), the *zntA*-deleted strain LMG194(*zntA*::*cat*) (×), and the deleted strain transformed with plasmids containing wtZntA (○), C392A (■), C392S (□), C392H (◆), C394A (◇), C394S (▲), and C394H (△). Cells were grown at 37 °C in a low phosphate medium in the absence and presence of different concentrations of (A) lead acetate, (B) zinc chloride, and (C) cadmium chloride. Cell growth was monitored after 24 h by measuring the absorbance at 600 nm.

Protein concentrations were determined using the bicinchoninic acid reagent with bovine serum albumin as standard.

Phosphorylation of the purified proteins with [γ-^{32}P]ATP was carried out as described earlier for 20 s at 37 °C with 10 μM [γ-^{32}P]ATP (*29*). Acylphosphate formation using [^{32}P]-Pi was carried out with 10 μg of purified proteins and 20 μM [^{32}P]Pi with or without the appropriate metal salt solution at 30 μM concentration for 10 min at 37 °C (*20*). The reactions were stopped with 10% TCA. For blank samples, the stop solution was added before the addition of [γ-^{32}P]ATP or [^{32}P]Pi.

To test whether prebinding metal ion to ZntA or ΔN-ZntA, a mutant that lacks the N-terminal domain and the N-terminal metal-binding site, in the absence of nucleotides results in inactivation of the protein, assays were performed as follows (*31*). Using the same protocol used to prepare samples for stoichiometry measurements with ICP-MS, ZntA and ΔN-ZntA were bound to different metal ions. wtZntA binds two metal ions, while ΔN-ZntA binds a single metal ion, with high affinity (*20*). Following removal of all unbound or weakly bound metal ions using consecutive Sephadex G-25 columns, the ATPase activity was assayed using the coupled assay system, except that no additional Pb^{2+}, Zn^{2+}, or Cd^{2+} was added. Approximately 4 μM (final concentration) wtZntA or ΔN-ZntA bound to different metal ions was added to the assay buffer, and the assay was initiated with the addition of ATP.

RESULTS

The in Vivo Resistance Activity of the Cys392 and Cys394 Mutants to Pb^{2+}, Zn^{2+}, and Cd^{2+} in the Growth Medium. The sensitivity of the *zntA*-deleted strain, LMG194(*zntA*::*cat*), to toxic levels of metal salts in the growth medium can be complemented by *wtzntA*. The ability of the individual mutations at Cys392, Cys394, and P393A to confer resistance to LMG194(*zntA*::*cat*) against toxic levels of Pb^{2+}, Cd^{2+}, and Zn^{2+} in the growth medium was tested. The C392A and C394A were not able to confer resistance against Pb^{2+}, Zn^{2+}, and Cd^{2+} (Figure 2A−C) and were indistinguishable in their growth profile from the *zntA*-deleted strain. Also, the conservative histidine and serine substitutions at Cys392 and Cys394 were unable to confer any resistance to Pb^{2+} (Figure 2A). However, the serine and histidine mutants (C392H, C392S, C394H, and C394S) were able to provide partial resistance to Zn^{2+} and Cd^{2+}, though the activity was much less compared with wtZntA (Figure 2B,C). Figure 2 shows growth of the different strains after 24 h; a similar trend was observed at 30 h of growth (not shown). The P393A mutant was unable to confer resistance to any concentration of Pb^{2+}, Zn^{2+}, and Cd^{2+} (data not shown).

Activity of the Purified Cys392 and Cys394 Mutants. For the serine and histidine substitutions at Cys392 and Cys394, levels of expression of the mutant proteins with or without histidyl tags were similar to that of wtZntA; for the alanine substitutions, the levels were slightly lower. P393A was expressed to only 5−10% of wtZntA levels. The ATPase activity was measured for wtZntA and the mutants for the metal ions Pb^{2+}, Zn^{2+}, Cd^{2+}, Cu^{2+}, Ni^{2+}, and Co^{2+}. The assay protocol was modified to remove DTT from the enzyme prior to the assays to ensure that none of the metal ions, especially Cu^{2+}, was reduced during the assay. As we have reported before, Pb^{2+}, Zn^{2+}, or Cd^{2+} salts can stimulate the ATP hydrolysis activity of wtZntA, with Pb^{2+} displaying the highest activity (*24*). By the modified assay, three other divalent metal ions (Cu^{2+}, Ni^{2+}, and Co^{2+}) were also shown to weakly stimulate the ATPase activity of wtZntA. Table 1 shows that for wtZntA the activity with Cu^{2+} or Ni^{2+} is just slightly lower than that of Cd^{2+}, while Co^{2+} has the lowest ATPase activity of the six cations. We reported previously that thiolates of cysteine in the assay medium increase the ATPase activity of ZntA 4−8-fold with Pb^{2+}, Zn^{2+}, and Cd^{2+} (Table 1); the activity in the presence of thiolates is probably a more accurate representation of the in vivo activity (*24*). Thiolates increased the activity with Co^{2+} and Ni^{2+} 2−3-fold. By comparison of the activity due to various metals, especially in the presence of thiolates, it is clear that ZntA is highly selective for one group of substrates (Pb^{2+}, Zn^{2+}, and Cd^{2+}) over the other (Cu^{2+}, Ni^{2+}, and Co^{2+}) (Table 1). It should be noted that the K_m's in Table 1 are apparent K_m's, which take into account the total metal ion concentration in the buffer. This is in contrast to the association constants for metal binding, K_a's in Table 3, which take into account only the free metal ion concentration in the buffer.

The alanine substitutions at Cys392, Cys394, and Pro393—C392A, Cys394A, and P393A—showed no measurable activity with any cation. Pb^{2+}, the best substrate for ZntA,

Table 1. Kinetic Parameters Obtained for the Histidine and Serine Substitutions at Cys392 and Cys394 at 37 °C for Different Divalent Metal Ions[a]

	wtZntA		C392H		C392S		C394H		C394S		C392H/C394H		C392S/C394S	
	V_m	K_m	V_m	K_m	V_m	K_m	V_m	K_m	V_m	K_m	V_m	K_m	V_m	K_m
Pb^{2+}	638 ± 3	6.1 ± 0.5	*b*		*b*	*b*	*b*		37 ± 0.4	14 ± 0.6	*b*		*b*	
Zn^{2+}	210 ± 3	5.1 ± 0.3	31 ± 0.3	10 ± 0.4	36 ± 0.4	9 ± 0.4	25 ± 0.1	12 ± 0.3	23 ± 0.2	9 ± 0.4	11 ± 0.4	13 ± 1.6	11 ± 0.1	7 ± 0.4
Cd^{2+}	102 ± 1	3.1 ± 0.2	21 ± 0.3	12 ± 0.7	28 ± 0.2	11 ± 0.4	19 ± 0.3	10 ± 0.6	8 ± 0.1	7 ± 0.2	11 ± 0.2	10 ± 1.0	12 ± 0.3	13 ± 1.1
Cu^{2+}	85 ± 2	3.4 ± 0.3	18 ± 0.2	13 ± 0.7	10 ± 0.2	10 ± 0.1	14 ± 0.1	13 ± 0.4	12 ± 0.1	7 ± 0.3	13 ± 0.4	10 ± 1.2	6 ± 0.4	19 ± 3.6
Ni^{2+}	76 ± 1	2.1 ± 0.2	14 ± 0.2	13 ± 0.8	17 ± 0.2	13 ± 1	10 ± 0.2	9 ± 0.7	12 ± 0.1	7 ± 0.3	11 ± 0.3	13 ± 1.2	*b*	
Co^{2+}	36 ± 1	4.0 ± 0.3	8 ± 0.1	7 ± 0.5	12 ± 0.3	12 ± 1	8 ± 0.1	8 ± 0.4	11 ± 0.1	7 ± 0.2	6 ± 0.2	14 ± 2.1	9 ± 0.2	18 ± 1.3
Pb^{2+} + thiolate	2497 ± 48	150 ± 10	*b*		*b*	*b*	*b*		*b*		*b*		*b*	
Zn^{2+} + thiolate	932 ± 5	105 ± 1	145 ± 5	131 ± 14	196 ± 4	141 ± 8	113 ± 4	131 ± 12	167 ± 4	182 ± 12	59 ± 2	83 ± 9	41 ± 2	99 ± 12
Cd^{2+} + thiolate	862 ± 5	123 ± 8	106 ± 2	114 ± 8	106 ± 2	148 ± 9	103 ± 2	110 ± 8	100 ± 2	152 ± 10	61 ± 1	91 ± 7	38 ± 1	139 ± 8
Cu^{2+} + thiolate	104 ± 2	85 ± 8	33 ± 1	158 ± 9	26 ± 1	124 ± 15	35 ± 1	171 ± 15	25 ± 1	145 ± 20	53 ± 3	105 ± 17	30 ± 1	127 ± 13
Ni^{2+} + thiolate	138 ± 7	169 ± 27	63 ± 2	80 ± 9	73 ± 2	80 ± 7	64 ± 2	83 ± 9	57 ± 1	117 ± 9	41 ± 1	116 ± 9	*b*	
Co^{2+} + thiolate	103 ± 3	75 ± 11	45 ± 1	133 ± 11	56 ± 1	126 ± 5	36 ± 1	92 ± 10	55 ± 1	104 ± 8	29 ± 1	66 ± 9	28 ± 1	96 ± 13

[a] Assays were performed in the absence and presence of the thiolate form of cysteine present at a concentration equal to the metal ion concentration. No activity was observed for C392A, C394A, and P393A for any metal ion, as also with Pb^{2+} for all the mutants. Assay conditions are described in Experimental Procedures. V_m values are in nmol/(mg·min) and apparent K_m values are in μM. [b] No activity detected.

showed no activity with the histidine or serine substitutions at Cys392 and Cys394. These in vitro results support the in vivo resistance activity of the Cys392 and Cys394 mutants.

The mutants where histidine replaces either or both of the two cysteines—C392H, C394H, and C392H/C394H—had diminished but still measurable activity with Zn^{2+}, Cd^{2+}, Ni^{2+}, Cu^{2+}, and Co^{2+}. For C392H and C394H, the activity was ~4−8-fold lower relative to wtZntA, in the absence of thiolates, while the apparent K_m's were slightly higher. In the presence of thiolates, the activity with Zn^{2+} and Cd^{2+} was 6−8-fold lower compared with wtZntA. Activity with Ni^{2+}, Co^{2+}, and Cu^{2+} was only ~2−3-fold lower. The C392H/C394H double mutant had 2−3-fold lower activity with Zn^{2+} and Cd^{2+} than the single histidine mutants, though its activity with Cu^{2+}, Ni^{2+}, and Co^{2+} was similar to that of the single mutants.

Single serine substitutions at residues 392 and 394 also resulted in a 3−8-fold decrease in activity for all five cations (Zn^{2+}, Cd^{2+}, Ni^{2+}, Cu^{2+}, and Co^{2+}) and no activity with Pb^{2+}. In the presence of thiolates, the decrease in activity was only 2-fold for Co^{2+} and Ni^{2+} but 4−8-fold for Zn^{2+}, Cu^{2+}, and Cd^{2+}. The serine double mutant, C392S/C394S, showed no activity with Ni^{2+}. Also, similar to the histidine double mutant at residues 392 and 394, it showed 2−4-fold lower activity with Zn^{2+} and Cd^{2+} than the single serine mutants; its activity with Cu^{2+} and Co^{2+} was similar to that of the single mutants.

Acylphosphate Intermediate Formation for ZntA and the ^{392}CPC^{394} Mutants. P-type ATPases form a covalent acylphosphate intermediate during the transport cycle. In ZntA, following metal ion binding, ATP is hydrolyzed to ADP in the forward direction, together with the transfer of the γ-phosphate group to an invariant aspartate residue (*32*). In the reverse direction, ZntA and other P-type ATPases can also form the acylphosphate intermediate in the presence of inorganic phosphate; the reverse phosphorylation occurs in the absence of metal ion binding and is inhibited by metal binding. The inactive ^{392}CPC^{394} mutants—C392A, C394A, and P393A—showed no acylphosphate formation with ATP; the other mutants showed low levels of the intermediate, only in the presence of Zn^{2+}, Cd^{2+}, Cu^{2+} Ni^{2+}, and Co^{2+} (data not shown). All the mutants, including the completely inactive ones, were able to form the intermediate with [^{32}P]-Pi in the absence of metal ions; like wtZntA, the steady-state levels of intermediate generated were ~1 nmol/mg of protein (data not shown). The inactive mutants (C392A, C394A, and P393A) showed no change in the acylphosphate levels formed with Pi in the presence of metal ions. The other mutants showed decreased levels of the intermediate when Zn^{2+}, Cd^{2+}, Cu^{2+}, Ni^{2+}, and Co^{2+} were present. Since all the mutants were quite competent in catalyzing this partial reaction, their decreased activity or complete inactivity with respect to ATP hydrolysis or in vivo resistance is not due to protein misfolding.

Stoichiometry of Metal Binding to ^{392}CPC^{394} Mutants using ICP-MS. The effect of the mutations on metal binding was tested by measuring the stoichiometry of bound metals by ICP-MS (Table 2). wtZntA can bind two metal ions with high affinity, one in the N-terminal domain and a second in the transmembrane domain (*19*, *20*). Binding stoichiometry for C392A, C394A, and P393A was ~1 for all six metals, confirming that these mutants are unable to bind any of the

Table 2. Stoichiometry of Metal Bound to the ^{392}CPC^{394} Mutants Using ICP-MS[a]

	lead	cadmium	zinc	cobalt	nickel	copper
wtZntA[b]	1.8 ± 0.1	2.2 ± 0.0	1.9 ± 0.0	2.1 ± 0.3	1.9 ± 0.3	1.8 ± 0.4
C392A	1.0 ± 0.01	1.0 ± 0.01	1.0 ± 0.1	1.0 ± 0.04	1.2 ± 0.02	1.1 ± 0.1
C392H	1.0 ± 0.1	2.0 ± 0.1	1.9 ± 0.01	2.2 ± 0.01	2.3 ± 0.06	2.3 ± 0.0
C392S	1.0 ± 0.0	1.9 ± 0.0	2.0 ± 0.0	2.0 ± 0.04	2.1 ± 0.0	2.2 ± 0.1
C394A	0.9 ± 0.0	1.0 ± 0.1	0.9 ± 0.2	1.0 ± 0.06	1.0 ± 0.01	0.8 ± 0.1
C394H	1.0 ± 0.0	2.0 ± 0.2	1.8 ± 0.0	2.0 ± 0.07	1.9 ± 0.03	1.8 ± 0.07
C394S	0.9 ± 0.1	1.8 ± 0.1	1.8 ± 0.1	1.8 ± 0.04	1.9 ± 0.01	2.0 ± 0.0
C392H/C394H	1.0 ± 0.2	2.0 ± 0.3	2.1 ± 0.2	1.7 ± 0.2	1.9 ± 0.02	2.1 ± 0.2
C392S/C394S	1.0 ± 0.1	1.8 ± 0.2	2.0 ± 0.3	1.7 ± 0.2	0.9 ± 0.2	2.0 ± 0.4
P393A	0.9 ± 0.1	1.0 ± 0.1	0.8 ± 0.1	0.9 ± 0.1	0.9 ± 0.1	1.0 ± 0.01

[a] Samples were prepared as described in Experimental Procedures. [b] From ref *20*.

metals in the transmembrane domain. All the mutants, including the serine and histidine substitutions, showed a stoichiometry of one with lead, confirming that they had lost the ability to bind lead at the transmembrane site (Table 2). On the other hand, the stoichiometry for the serine and histidine single and double mutants for the other five metals—cadmium, zinc, cobalt, nickel, and copper, was 1.8−2.3, indicating that they were capable of binding these metals at both the transmembrane and the N-terminal sites. However, the serine double mutant C392S/C394S showed a stoichiometry of 1 with Ni^{2+}.

Activity of wtZntA with Metal Bound in the Absence of Nucleotides. For stoichiometry measurements using ICP-MS, ZntA and the mutants were incubated with metal ions in the absence of any nucleotides followed by removal of excess metal ions, as well as weakly bound metal ions, by column chromatography. It is possible that ZntA has a low-affinity metal-binding site in the transmembrane domain, in addition to the high-affinity site, which is essential for overall activity of the protein. We therefore tested whether the metal-bound sample prepared for ICP-MS measurements retained activity in the absence of any extra metal ions. Samples of ZntA and ΔN-ZntA, a truncation mutant of ZntA that lacks the N-terminal domain and has only the single metal-binding site in the transmembrane domain, were prepared exactly as for the stoichiometry measurements. ZntA had 2 equiv of bound metal ion, and ΔN-ZntA had 1 equiv. The samples (∼4 μM final concentration of protein) were then assayed for ATPase activity without the addition of any extra soft metal ion to the assay buffer (Figure 3); they showed ATPase activity with different metal ions. Control experiments were carried out to ensure that the metal remained bound to the protein during the incubation in the assay buffer, prior to the start of the assay by addition of ATP. This shows that ZntA tightly bound to metal ions in the absence of nucleotides retains overall activity.

Affinity of Zn^{2+}, Pb^{2+}, and Cd^{2+} for the Transmembrane Site in the ^{392}CPC^{394} Mutants Using Mag-fura-2. Since the histidine and serine substitutions at residues 392 and 394 were capable of binding metals yet had low overall activity relative to wtZntA, their metal binding affinity was determined. Competition titration with the metal ion indicator and chelator mag-fura-2 was carried out with purified, reduced mutant proteins as described in detail earlier (*19*, *20*). The data was fitted to a one- or two-binding-sites model as described previously (*29*) using the software Dynafit (*33*); the affinity of the buffer Bis-Tris for metal ions was taken into account (*34*).

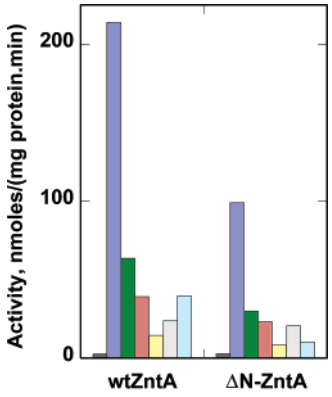

FIGURE 3: ATPase activity with purified wtZntA and ΔN-ZntA using pre-metal-bound protein in the absence of any metal salt solutions at 37 °C and pH 7.0. wtZntA and ΔN-ZntA were bound to different metal ions as described in the Experimental Procedures. Excess metal ions were then removed. Approximately 4 μM (final concentration) metal-bound protein was incubated in the assay buffer with 2.5 mM $MgCl_2$ for 5 min before starting the reaction with the addition of 2.5 mM ATP. Reactions were carried out for 10 min. From left to right, the bars denote protein bound to no metal, Pb^{2+}, Zn^{2+}, Cd^{2+}, Co^{2+}, Cu^{2+}, and Ni^{2+}.

$$E + M^{2+} \overset{K_1E}{\longleftrightarrow} E{\cdot}M^{2+} \quad (1)$$

$$E{\cdot}M^{2+} + M^{2+} \overset{K_2E}{\longleftrightarrow} E{\cdot}(M^{2+})_2 \quad (2)$$

$$I + M^{2+} \overset{K_I}{\longleftrightarrow} I{\cdot}M^{2+} \quad (3)$$

where E is the protein and I is the indicator, mag-fura-2. The association constants of mag-fura-2 for Zn^{2+}, Cd^{2+}, and Pb^{2+} used in these fits were determined previously; they were 5.2×10^7, 2.5×10^7, and 3.1×10^8 M^{-1} for Zn^{2+}, Cd^{2+}, and Pb^{2+}, respectively (*20*, *35*). Figure 4A−F shows the decrease in absorbance at 366 nm versus the metal ion concentration and the fits to the data for the Cys392 and Cys394 single mutants (similar sets of data were obtained for P393A, C392H/C394H, and C392S/C394S). Consistent with the ICP-MS data, C392A, C394A, and P393A showed only one binding site for Zn^{2+}, Cd^{2+}, and Pb^{2+}; attempts to fit the data for these proteins to two binding sites resulted in a second association constant in the molar range. For Zn^{2+} and Cd^{2+}, the serine and histidine mutants showed two binding sites, as previously observed for wtZntA as well. Table 3, section A, summarizes the association constants obtained for the metal binding sites for the Cys392, Cys394, and the P393A mutants; the values for wtZntA are also included. The association constants obtained with the mutants are similar to those obtained for wtZntA for all three cations,

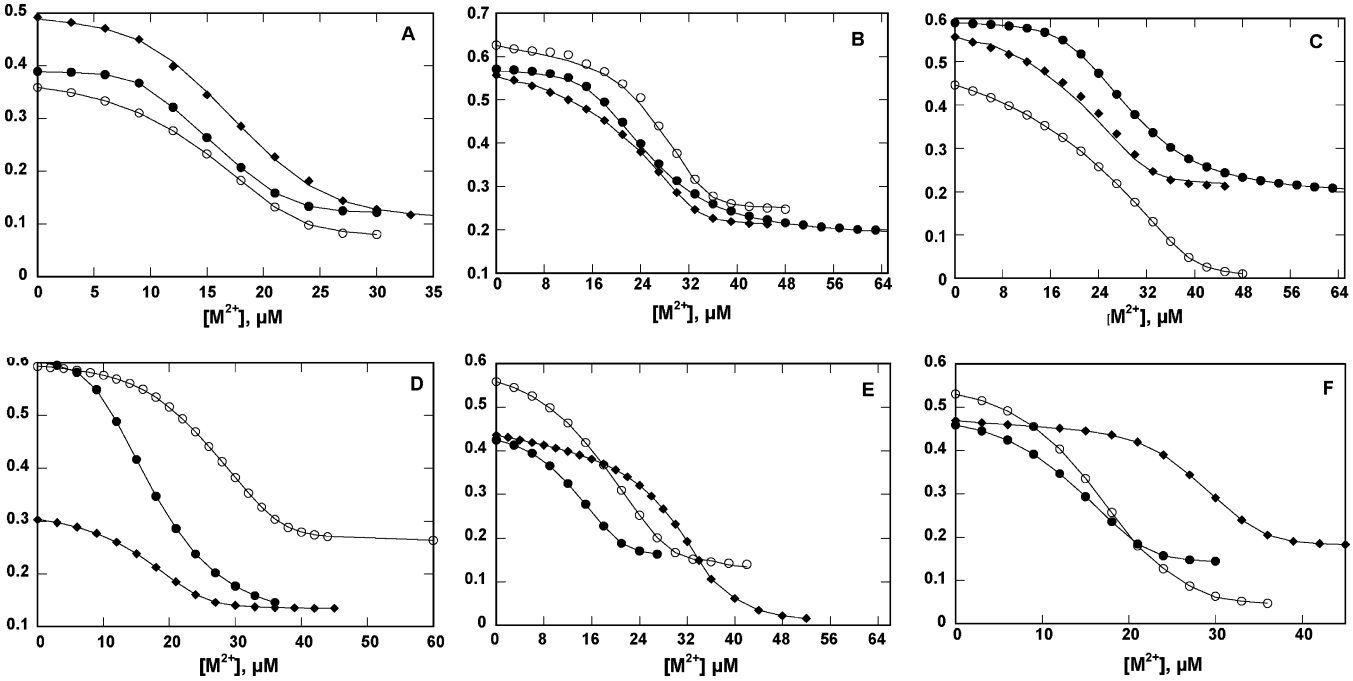

FIGURE 4: Plot of the absorbance change at 366 nm when increasing concentrations of metal salt solutions were added to mag-fura-2 and the Cys392 and Cys394 mutants in 10 mM Bis-Tris and 0.5 mM DDM, pH 7.0, and 20 °C: (A) C392A; (B) C392H; (C) C392S; (D) C394A; (E) C394H; (F) C394S; (●) Pb^{2+}; (○) Zn^{2+}; (◆) Cd^{2+}. Data were fitted as described in the Results section. The protein and indicator concentrations used were as follows: (A) ~11, 11, and 15 μM C392A for Pb^{2+}, Zn^{2+}, and Cd^{2+}, respectively, with ~15 μM mag-fura-2; (B) ~19, 8, and 10 μM C392H for Pb^{2+}, Zn^{2+}, and Cd^{2+}, respectively, with ~20 μM mag-fura-2; (C) ~18, 11, and 10 μM C392S for Pb^{2+}, Zn^{2+}, and Cd^{2+}, respectively, with ~20 μM mag-fura-2 for Pb^{2+} and Zn^{2+} and 15 μM for Cd^{2+}; (D) ~18, 12, and 11 μM C394A for Pb^{2+}, Zn^{2+}, and Cd^{2+}, respectively, with ~16 μM mag-fura-2 for Pb^{2+} and Zn^{2+} and 8 μM for Cd^{2+}; (E) ~13, 7, and 15 μM C394H for Pb^{2+}, Zn^{2+}, and Cd^{2+}, respectively, with ~12 μM mag-fura-2 for Pb^{2+} and Cd^{2+} and 16 μM for Zn^{2+}; (F) ~11, 8, and 12.5 μM C394S for Pb^{2+}, Zn^{2+}, and Cd^{2+}, respectively, with ~13 μM mag-fura-2 for Pb^{2+} and Cd^{2+} and 15 μM for Zn^{2+}.

indicating that the affinity for either the N-terminal site or the transmembrane site is not significantly altered by the substitutions.

Affinity of the Two Metal Sites in wtZntA and the ^{392}CPC^{394} Mutants Using Tryptophan Fluorescence Quenching. ZntA has six tryptophan residues, of which Trp52 is located in the N-terminal domain close to the N-terminal metal binding site in primary sequence. The other five are distributed over the rest of the protein sequence. Metal binding to the isolated N-terminal domain produces ~20−25% quenching of the fluorescence due to Trp52 (S. J. Dutta and B. Mitra, unpublished observations). Metal binding to the transmembrane site in ΔN-ZntA, a ZntA mutant that lacks the N-terminal domain, produces ~10−15% quenching of fluorescence due to one or more of the other five tryptophan residues since Trp52 is missing in this mutant (*20*). The smaller degree of fluorescence quenching upon metal binding to the transmembrane site is possibly because the majority of the five tryptophan residues in ΔN-ZntA are not affected by cation binding to the transmembrane site. Nevertheless, it is clear that metal binding to both the N-terminal and transmembrane sites in isolated ZntA fragments produces quenching of the native fluorescence of distinct tryptophan residues. This intrinsic fluorescence quenching provides a useful tool to measure the affinity of different divalent metal ions to both sites in full-length wtZntA and the ^{392}CPC^{394} mutants. Figure 5A shows a titration of wtZntA with increasing concentrations of zinc chloride in the presence of ~5 μM EDTA as a metal ion competitor; the fluorescence was quenched ~40−45%. Similar decreases in tryptophan fluorescence emission were observed for other divalent metal ions as well. Changes in fluorescence intensity at 340 nm were plotted versus different divalent metal ion concentration in Figure 5B. It should be noted that in this equilibrium titration experiment, the degree of fluorescence quenching is saturated at a metal concentration equal to the sum of the EDTA concentration and twice that of the wtZntA concentration, indicating that there are two metal sites on wtZntA, supporting our stoichiometry measurements done under nonequilibrium conditions. The data were fitted to the two-site metal-binding model as noted above using Dynafit. For the fitting, the affinity of the buffer Bis-Tris for metals was taken into account (*34*), as well as the affinity of EDTA (~5 μM) for the different metal ions (*36*). Table 3, section B, lists the association constants obtained for the two sites in wtZntA for six different cations using this method. wtZntA has the highest affinity for Pb^{2+} and Cu^{2+}, followed by ~10-fold lower affinity for Cd^{2+}, Zn^{2+}, Ni^{2+}, and Co^{2+}.

Using similar titrations, we determined the association constants of the ^{392}CPC^{394} mutants for Pb^{2+}, Cd^{2+}, Zn^{2+}, Cu^{2+}, Co^{2+}, and Ni^{2+} (Table 3, section B). Figure 6 shows data for the single cysteine mutants. Similar data was obtained for P393A, C392H/C394H, and C392S/C394S (not shown). As observed with the titration experiments using mag-fura-2 as an indicator and also the ICP-MS data, C392A, C394A, and P393A lost the ability to bind a second metal ion. Also, none of the mutants were able to bind a second Pb^{2+} ion. The serine and histidine substitutions at Cys392 and Cys394 could bind two Zn^{2+}, Cd^{2+}, Ni^{2+}, Cu^{2+}, and Co^{2+} cations, with the exception of C392S/C394S, which could only bind one Ni^{2+}. The association constants for all the mutant proteins obtained by this method for Pb^{2+}, Cd^{2+}, and

Table 3. Association Constants for the Binding of Different Metal Ions to wtZntA and the Mutants at Cys392 and Cys384[a]

A. Using Competition Titration with Mag-fura-2

	lead	cadmium	zinc
wtZntA[b]	$(1.3 \pm 0.1) \times 10^9$	$(1.3 \pm 0.1) \times 10^8$	$(1.1 \pm 0.1) \times 10^8$
	$(4.5 \pm 0.01) \times 10^9$	$(5.0 \pm 0.2) \times 10^8$	$(5.0 \pm 0.1) \times 10^8$
C392A	$(1.7 \pm 0.01) \times 10^9$	$(1.5 \pm 0.03) \times 10^8$	$(1.3 \pm 0.01) \times 10^8$
C392H	$(4.7 \pm 0.3) \times 10^9$	$(1.2 \pm 0.01) \times 10^8$	$(1.4 \pm 0.01) \times 10^8$
		$(2.8 \pm 0.01) \times 10^8$	$(2.1 \pm 0.01) \times 10^8$
C392S	$(4.4 \pm 0.4) \times 10^9$	$(1.3 \pm 0.01) \times 10^8$	$(1.6 \pm 0.01) \times 10^8$
		$(2.2 \pm 0.01) \times 10^8$	$(3.2 \pm 0.02) \times 10^8$
C394A	$(2.2 \pm 0.3) \times 10^9$	$(1.1 \pm 0.01) \times 10^8$	$(2.3 \pm 0.1) \times 10^8$
C394H	$(1.3 \pm 0.01) \times 10^9$	$(1.1 \pm 0.01) \times 10^8$	$(1.5 \pm 0.01) \times 10^8$
		$(5.0 \pm 0.01) \times 10^8$	$(4.2 \pm 0.06) \times 10^8$
C394S	$(2.0 \pm 0.01) \times 10^9$	$(1.7 \pm 0.01) \times 10^8$	$(1.7 \pm 0.01) \times 10^8$
		$(3.4 \pm 0.01) \times 10^8$	$(3.6 \pm 0.02) \times 10^8$
C392H/C394H	$(6.1 \pm 0.6) \times 10^9$	$(2.6 \pm 0.46) \times 10^8$	$(2.6 \pm 0.07) \times 10^8$
		$(2.9 \pm 0.27) \times 10^8$	$(8.1 \pm 0.58) \times 10^8$
C392S/C394S	$(1.8 \pm 0.20) \times 10^9$	$(2.7 \pm 1.1) \times 10^8$	$(2.6 \pm 0.03) \times 10^8$
		$(1.3 \pm 0.01) \times 10^8$	$(6.0 \pm 0.21) \times 10^8$
P393A	$(6.1 \pm 0.62) \times 10^9$	$(2.6 \pm 0.01) \times 10^8$	$(2.6 \pm 0.23) \times 10^8$

B. By Direct Fluorescence Quenching

	lead	cadmium	zinc	cobalt	nickel	copper
wtZntA	$(6.8 \pm 0.01) \times 10^9$	$(4.0 \pm 0.01) \times 10^8$	$(4.0 \pm 0.01) \times 10^8$	$(1.9 \pm 0.05) \times 10^8$	$(4.0 \pm 0.01) \times 10^8$	$(2.0 \pm 0.01) \times 10^9$
	$(4.1 \pm 1.3) \times 10^9$	$(1.3 \pm 0.01) \times 10^8$	$(2.4 \pm 0.02) \times 10^8$	$(6.7 \pm 0.01) \times 10^7$	$(2.4 \pm 0.40) \times 10^8$	$(2.9 \pm 0.04) \times 10^9$
C392A	$(1.8 \pm 0.01) \times 10^9$	$(1.9 \pm 0.01) \times 10^8$	$(2.7 \pm 0.01) \times 10^8$	$(4.3 \pm 0.01) \times 10^8$	$(3.1 \pm 0.01) \times 10^8$	$(2.0 \pm 0.01) \times 10^9$
C392H	$(2.3 \pm 0.01) \times 10^9$	$(2.8 \pm 0.01) \times 10^8$	$(2.4 \pm 0.01) \times 10^8$	$(1.9 \pm 0.23) \times 10^8$	$(2.9 \pm 0.41) \times 10^8$	$(2.7 \pm 0.01) \times 10^9$
		$(1.4 \pm 0.05) \times 10^8$	$(8.6 \pm 2.5 \times 10^8$	$(2.6 \pm 0.01) \times 10^7$	$(5.3 \pm 1.1) \times 10^8$	$(2.6 \pm 0.01) \times 10^9$
C392S	$(2.2 \pm 0.01) \times 10^9$	$(2.1 \pm 0.01) \times 10^8$	$(2.4 \pm 0.02) \times 10^8$	$(1.5 \pm 0.04) \times 10^8$	$(2.6 \pm 0.16) \times 10^8$	$(1.8 \pm 0. 10) \times 10^9$
		$(2.6 \pm 0.03) \times 10^8$	$(4.0 \pm 0.01) \times 10^8$	$(7.3 \pm 2.6) \times 10^7$	$(3.8 \pm 0.05) \times 10^8$	$(2.3 \pm 0.15) \times 10^9$
C394A	$(9.0 \pm 0.19) \times 10^9$	$(2.4 \pm 0.01) \times 10^8$	$(2.4 \pm 0.01) \times 10^8$	$(3.8 \pm 0.03) \times 10^8$	$(2.4 \pm 0.13) \times 10^8$	$(3.9 \pm 0.09) \times 10^9$
C394H	$(2.1 \pm 0.01) \times 10^9$	$(2.0 \pm 0.01) \times 10^8$	$(1.3 \pm 0.01) \times 10^8$	$(5.9 \pm 1.1) \times 10^8$	$(2.7 \pm 0.01) \times 10^8$	$(2.4 \pm 0.01) \times 10^9$
		$(3.6 \pm 0.02) \times 10^8$	$(1.7 \pm 0.01) \times 10^8$	$(6.1 \pm 0.01) \times 10^7$	$(2.7 \pm 0.15) \times 10^8$	$(5.6 \pm 0.01) \times 10^9$
C394S	$(2.1 \pm 0.01) \times 10^9$	$(2.7 \pm 0.01) \times 0^8$	$(1.9 \pm 0.09) \times 10^8$	$(1.9 \pm 0.19) \times 10^8$	$(2.9 \pm 0.01) \times 10^8$	$(1.8 \pm 0.15) \times 10^9$
		$(6.2 \pm 0.48) \times 10^8$	$(4.8 \pm 0.69) \times 10^8$	$(7.8 \pm 0.37) \times 10^7$	$(6.5 \pm 1.8) \times 10^8$	$(7.4 \pm 2.4) \times 10^9$
C392H/C394H	$(1.4 \pm 0.01) \times 10^9$	$(4.0 \pm 0.06) \times 10^8$	$(1.6 \pm 0.01) \times 10^8$	$(1.3 \pm 0.02) \times 10^7$	$(1.4 \pm 0.01) \times 10^8$	$(1.6 \pm 0.06) \times 10^9$
		$(3.6 \pm 0.05) \times 10^8$	$(1.5 \pm 0.01) \times 10^8$	$(1.5 \pm 0.06) \times 10^7$	$(8.3 \pm 0.39) \times 10^8$	$(1.5 \pm 0.16) \times 10^9$
C392S/C394S	$(4.6 \pm 0.25) \times 10^9$	$(5.7 \pm 2.5) \times 10^8$	$(4.7 \pm 2.1) \times 10^8$	$(5.9 \pm 2.7) \times 10^7$	$(1.5 \pm 0.03) \times 10^8$	$(1.0 \pm 0.02) \times 10^8$
		$(3.1 \pm 0.05) \times 10^8$	$(8.3 \pm 3.6) \times 10^8$	$(4.3 \pm 0.01) \times 10^7$		$(6.1 \pm 0.8) \times 10^8$

[a] Units are in M^{-1}. Protein samples were prepared as described in Experimental Procedures. Data were fitted using Dynafit (*31*) with the assumption of two binding sites, except for C392A, C394A, and P393A, where only one binding site was assumed in the fit. This was also true for C392H, C392S, C394H, and C394S with Pb^{2+}. For these, fitting the data using a two-binding-site model yielded an unrealistically low value for the second association constant. [b] From ref *29*.

Zn^{2+} were similar to that of wtZntA and support the data obtained by titration with mag-fura-2. With Co^{2+}, Cu^{2+}, and Ni^{2+}, the same trend was observed; the mutations did not affect the affinity for these metal ions to a significant extent though the C392S/C394S mutant showed slightly lower affinity for Cu^{2+} (Table 3, section B).

DISCUSSION

P_{1B}-type ATPases are highly selective for the metal ions that they transport. Though only a few P_{1B}-type ATPases have been biochemically characterized with respect to metal selectivity, it is apparent that pumps with confirmed selectivity for Pb^{2+}, Cd^{2+}, Zn^{2+}, Cu^{2+}, Cu^{+}, and Co^{2+} belong to separate subgroups defined by sequence alignment. It is expected that these subgroups contain strictly conserved residues within each that confer metal ion selectivity. P_{1B}-type ATPases contain metal binding sites in a hydrophilic domain located at the N-terminus, or alternatively at the C-terminus, and in the transmembrane domain. Both types of metal sites appear to have distinct conserved ligands that possibly confer metal selectivity. We show in this study that wtZntA displays much higher selectivity for Pb^{2+}, Cd^{2+}, and Zn^{2+}, over Cu^{2+}, Ni^{2+}, and Co^{2+}, with respect to metal-ion-stimulated ATPase activity. Interestingly, both the N-terminal and the transmembrane metal sites in ZntA have similar affinity for these different metal ions, which does not correlate with the metal selectivity displayed by the pump (*19*, *20*). It is evident that metal selectivity does not depend on ionic size, and the charge is invariant among divalent cations. In this work, mutants of the transmembrane metal-binding residues were characterized in order to examine how specific metal ligands affected metal selectivity.

P_{1B}-type ATPases have a conserved (C,S,T)P(C,H) motif in transmembrane segment six, with the central proline invariant in all P-type pumps. Pumps specific for Pb^{2+}, Cd^{2+}, Zn^{2+}, and Cu^{+} have the CPC motif, whereas those specific for Cu^{2+} and Co^{2+} have a CPH and SPC motif, respectively. The CPC motif in ZntA was changed to APC and CPA to evaluate the importance of each cysteine in metal selectivity and activity. It was also changed to SPC, CPS, HPC, CPH, HPH, and SPS to test whether the selectivity could be changed to that of Co^{2+} or Cu^{2+}. The motif was changed to CAC to examine the importance of the conserved Pro393.

Purified C392A and C394A (with an APC and a CPA motif, respectively) showed no metal-stimulated ATPase activity or acylphosphate formation activity with ATP. The

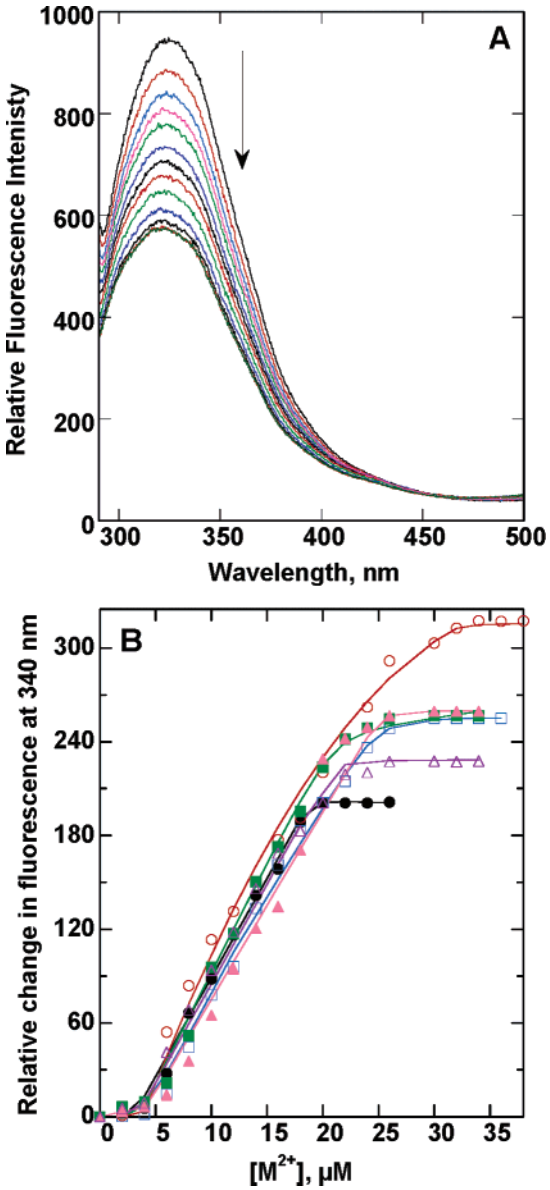

FIGURE 5: Panel A shows a decrease in fluorescence emission of wtZntA when increasing concentrations of zinc chloride were added to the protein in 10 mM BisTris, 0.5 mM DDM, and 5 μM EDTA, pH 7.0, and 20 °C. The excitation wavelength was 290 nm. Panel B shows plots of the relative change in fluorescence emission of wtZntA (~8−13 μM) at 340 nm as a function of the added metal salt concentration for different metal ions: (●) Pb^{2+}; (□) Zn^{2+}; (○) Cd^{2+}; (■) Co^{2+}; (△) Cu^{2+}; (▲) Ni^{2+}. The data was fitted as described in the Results section. The scale on the *y*-axis is in arbitrary units.

mutants were also completely inactive in vivo. These results are similar to those reported earlier for Cu^+-ATPases from *E. coli* and *A. fulgidus* (*25*, *26*). However, a recent study of CadA from *L. monocytogenes* reported that the C356A mutant (corresponding to a CPA motif) showed in vitro ATPase activity but no in vivo activity, in contrast to the C354A mutant (APC motif) (*28*). Given the close homology of Cu^+-ATPases and especially ZntA with CadA, the result with the CadA C356A mutant is unexpected. One reason for this different result could be that the ATPase assay on CadA, carried out on *Sf*9 membranes, is complicated by endogenous ATPase activity, varying levels of expression of the different mutants, and inhibitory effects of Cd^{2+} on the endogenous activity.

C392A and C394A in ZntA were unable to bind a metal ion at the transmembrane site with high affinity, under both equilibrium (for titration with metal ions) and nonequilibrium (ICP-MS measurements) conditions. Thus each of the residues flanking the proline is a ligand to the metal; even with one ligand missing, the transmembrane metal binding site is lost, and all activity is lost. The transmembrane site is thus essential for activity, unlike the N-terminal site; when the latter was knocked out or replaced by the corresponding domain from the Wilson Cu^+-ATPase, the resulting transporter was still functional (*19*, *31*, *37*).

C392H, C394H, C392S, C394S, and the serine and histidine double mutants have no activity with Pb^{2+}, either in vitro or in vivo. They are unable to bind Pb^{2+} at the transmembrane site. The oxygen of the serine hydroxyl side chain and the nitrogen from imidazole side chain of histidine, both relatively "hard" ligands, appear to be not suitable for binding Pb^{2+} in ZntA. We have shown that a strictly conserved aspartate residue in the middle of the eighth transmembrane segment in ZntA, Asp714, is a metal-binding ligand (*29*). Both this aspartate and its conservative replacement, glutamate, could bind Pb^{2+} with high affinity. Therefore, a carboxylate side chain is a suitable ligand for Pb^{2+}, but a hydroxyl side chain is not. From these observations, it is clear that the CPC motif is strictly essential for the selectivity toward Pb^{2+} in P_{1B}-type ATPases; even conservative substitutions are not tolerated. Binding of Pb^{2+} at the N-terminal site of ZntA is also different from that of other metal ions and possibly requires at least three cysteine residues (*19*, *38*). A recent EXAFS study suggests that in thiol-rich environments in proteins, Pb^{2+} binds with three-coordinate geometry whereas Zn^{2+} binds with four-coordinate geometry (*39*). Also, replacement of one of the cysteine ligands by a serine considerably weakened binding of Pb^{2+} relative to Zn^{2+} in metal-regulated transcription factors (*40*). In ZntA, it is possible that binding of Pb^{2+} has been optimized for thiol-rich environments at both the N-terminal and transmembrane sites and involves three-coordinate geometry; substitution of even one of the three ligands results in loss of binding.

C392H, C394H, and C392H/C394H were able to bind Cd^{2+}, Zn^{2+}, Cu^{2+}, Ni^{2+}, and Co^{2+} at the transmembrane site; the affinity for these metal ions is relatively unchanged from that of wtZntA. Thus, the imidazole side chain is a suitable ligand for these cations. Interestingly, these mutants did not show an increased affinity for Cu^{2+}. Despite the unaltered affinity for metal ions however, these mutants showed large reductions in metal-dependent ATP hydrolysis rates. The double mutant with the HPH motif shows lower activity with only Zn^{2+} and Cd^{2+} compared with the single histidine mutants, whereas its activity with Ni^{2+}, Cu^{2+}, and Co^{2+} is relatively unchanged. Thus, histidine substitutions at residues 392 and 394 destroy the predominant selectivity of wtZntA, and possibly other P_{1B}-type pumps, toward Pb^{2+}, Zn^{2+}, and Cd^{2+}. This is achieved through drastically lower binding affinity for Pb^{2+} but apparently more subtle effects in binding geometry for Zn^{2+} and Cd^{2+}, which are bound with unaltered affinity. Though Cu^{2+}-specific ATPases have a CPH motif in TM6, C394H did not show any enhanced selectivity for Cu^{2+}.

The single serine substitutions at Cys392 and Cys394 were able to bind Cd^{2+}, Zn^{2+}, Cu^{2+}, Ni^{2+}, and Co^{2+} at the

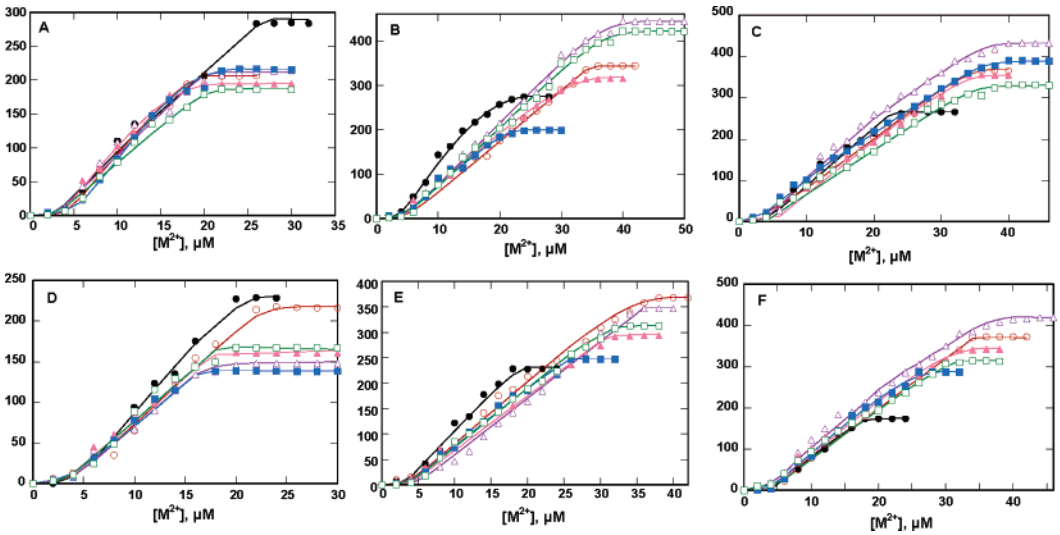

FIGURE 6: Plot of the changes in fluorescence emission intensity at 340 nm (excitation 290 nm) when increasing concentrations of metal salt solutions were added to the Cys392 and Cys394 mutants in 10 mM Bis-Tris, 0.5 mM DDM, and ~5 μM EDTA, pH 7.0, and 20 °C: (A) C392A (~13 μM for Zn^{2+}, Ni^{2+}, Cd^{2+}, Cu^{2+}, and Co^{2+} and ~19 μM for Pb^{2+}); (B) C392H (~8 μM for Zn^{2+}, 14 μM for Ni^{2+} and Cd^{2+}, and ~18 μM for Pb^{2+}, Cu^{2+}, and Co^{2+}); (C) C392S (~18 μM for Pb^{2+} and Cu^{2+}; ~15 μM for Cd^{2+}, Zn^{2+}, Ni^{2+}, and Co^{2+}); (D) C394A (~15 μM for Pb^{2+}; ~9 μM for Cd^{2+}; ~6 μM for Zn^{2+}, Ni^{2+}, Cu^{2+}, and Co^{2+}); (E) C394H (~15 μM for Pb^{2+}, Cd^{2+}, and Cu^{2+}; ~10−12 μM for Ni^{2+}, Co^{2+}, and Zn^{2+}); (F) C394S (~11−14 μM for Zn^{2+}, Pb^{2+}, Ni^{2+}, and Co^{2+}; ~15−17 μM for Cd^{2+} and Cu^{2+}); (●) Pb^{2+}; (○) Cd^{2+}; (△) Cu^{2+}; (▲) Ni^{2+}; (■) Zn^{2+}; (□) Co^{2+}. Data were fitted as discussed in the Results section.

transmembrane site with similar affinity to wtZntA. However, the double serine mutant, SPS, had a 10-fold lower affinity for Cu^{2+} and was unable to bind Ni^{2+} at the transmembrane site. With respect to metal-dependent ATPase activity, the serine mutants were similar to the histidine substitutions with decreased activity for all the metal ions relative to wtZntA, with the double mutant SPS showing lower activity with all the metals compared with the single serine mutants and no activity with Ni^{2+}. The hydroxyl oxygen of the serine side chain may not be a suitable ligand for these metal ions; possibly, the presence of at least one cysteine residue compensates for the serine in the single serine mutants. Serine substitutions at residues 392 and 394 destroyed the selectivity of wtZntA toward Pb^{2+}, Zn^{2+}, and Cd^{2+}. They did not show any increased selectivity for Co^{2+} with respect to binding affinity or activity, though in putative Co^{2+}-ATPases, the conserved motif is SPC.

P393A, with a CAC motif, was only expressed to 10% of wtZntA levels. This is possibly due to structural perturbations in transmembrane helix 6 caused by the loss of this proline. The purified protein showed no activity and was unable to bind a second metal ion unlike wtZntA, though it was still able to bind a cation in the N-terminal domain. This suggests that even though both cysteine residues were present, the optimal geometry for cation binding at the transmembrane site was lost. Our observations with P393A in ZntA are in contrast to those reported for the corresponding mutation, P355A, in CadA from *L. monocytogenes*, which retained some activity (*28*).

The results reported here with the ^{392}CPC^{394} mutants lend additional support to our earlier conclusion that metal-binding geometry plays an important role in addition to affinity in determining metal selectivity in these transporters (*20*). This may be the reason why the C392S and C394H mutants do not show increased selectivity for Co^{2+} and Cu^{2+}, respectively. Co^{2+}- and Cu^{2+}-selective ATPases have conserved residues besides the SPC and CPH motifs that may be ligands to the metal ion (*10*, *14*, *21*). It is likely that higher selectivity toward Cu^{2+} and Co^{2+} can only be achieved by changing these residues simultaneously together with those of the CPC motif.

While optimal metal-binding geometry appears to be an important parameter in determining selectivity, the results reported here for Pb^{2+} show that for some metal ions, certain residues are simply not suitable ligands for high-affinity binding. Mutants with these substitutions lose the ability to bind these cations with affinity high enough to effectively compete with weak ligands in the assay buffer. Thus, both binding affinity and optimal binding geometry play a role in metal selectivity in P_{1B}-type ATPases. In this context, mutagenesis studies of the Cu^+ transporters from *A. fulgidus*, *E. coli*, and yeast Ccc2p should be mentioned. For these pumps, the cysteines of the CPC motifs were mutated not only to alanines but also to CPS, SPC, and CPH. The CPS mutant in CopA from *A. fulgidus* did not show any ATPase activity (*26*). The CPH mutant in CopA from *E. coli* had no ATPase, acylphosphate formation, or in vivo resistance activity (*25*). This is in contrast to the histidine and serine mutations at Cys392 and Cys394 in ZntA, which had both in vivo resistance activity to Zn^{2+} and Cd^2 and in vitro ATPase activity with most cations. Metal binding was not measured for either of the CopA mutants, so it is not evident why they were completely inactive. One possibility is that Cu^+ behaves in the same way as Pb^{2+} does with the serine and histidine mutants in ZntA. Just as for Pb^{2+}, the CPC motif may be strictly required for binding Cu^+. On the other hand, it is also possible that Cu^+ is bound tightly by the mutants, but with a geometry that does not support efficient catalysis. Metal-binding measurements would help to answer this question.

The metal-binding studies reported here, both by ICP-MS (nonequilibrium conditions) and by metal titration (equilibrium conditions), show that wtZntA has two high-affinity metal-binding sites; one of these is in the membrane. Measurements of metal-binding rates at the N-terminal site show that metal ions have very high on rates and slow off

rates (*38*). It is likely that this is true for the transmembrane site also. It was suggested based on studies of mutations of the CPC motif in yeast Ccc2p and CadA from *L. monocytogenes* that these proteins have two metal binding sites in the transmembrane domain with each cysteine from the CPC motif contributing to a different metal site. While both the SPC and CPS mutants in Ccc2p showed no in vivo or ATPase activity, only the SPC mutant showed phosphorylation by ATP (*41*). In CadA, the APC mutant showed no ATPase activity, but the CPA mutant did (*28*). Metal binding was not directly studied for either of these two proteins or their different mutants, so the metal affinity of these sites is not known. Results reported here and earlier for ZntA strongly suggest that only one metal ion is bound to the transmembrane site in ZntA with high affinity. The discrepancy between our results and those reported for Ccc2p and CadA can be explained by the following hypothesis. During the actual reaction cycle of ZntA and related pumps, a single metal ion is bound to the transmembrane site in the E_1 state. In the E_2 state, metal ion release from this site to the periplasm is accompanied by metal transfer to it from the N-terminal metal site. The N-terminal site in ZntA can interact with the transmembrane site (S. J. Dutta and B. Mitra, manuscript in preparation). During this metal transfer/metal release process in the E_2 state, it is likely that the cysteines of the CPC motif behave differently, with one accepting the incoming metal ion from the N-terminal site while the other is in the process of releasing the outgoing metal ion. In this study, we have used the high-affinity transmembrane metal site in the E_1 state to investigate the basis of metal selectivity.

Conclusions. P_{1B}-type ATPases have a strictly conserved (C,S,T)P(C,H) motif in the sixth transmembrane segment. The identity of the residues flanking the proline depends on the metal selectivity of different subgroups of P_{1B}-type ATPases. In ZntA and its homologues that are selective for Pb^{2+}, Zn^{2+}, and Cd^{2+}, the motif is CPC. Conservative and nonconservative mutations at each of the two cysteines were characterized. All the mutants were competent in catalyzing acylphosphate formation in the reverse direction, indicating they were properly folded proteins. The alanine substitutions lost all metal-dependent activity and could not bind a metal ion at the transmembrane site, indicating the importance of each cysteine as a ligand to the metal ion. Serine and histidine substitutions lost the ability to bind Pb^{2+}, indicating that the cysteine residues are strictly necessary for binding Pb^{2+} with high affinity at the transmembrane site. Mutants with serine and histidine substitutions retained the ability to bind Zn^{2+}, Cd^{2+}, Cu^{2+}, Ni^{2+}, and Co^{2+} with high affinity but showed large decreases of in vivo metal resistance and in vitro ATP hydrolysis activity and loss of selectivity to Zn^{2+} and Cd^{2+}. The P393A mutant showed no activity and could not bind any metal ion at the transmembrane site, though it retained both cysteine residues. These observations indicate that metal selectivity in P_{1B}-type ATPases is achieved by selection of metal ligands that give rise to high binding affinity and, even more importantly, optimal binding geometry.

REFERENCES

1. Inesi, G. (1985) Mechanism of calcium transport, *Annu. Rev. Physiol. 47*, 573−601.
2. Axelson, K. B., and Palmgren, M. G. (1998) Evolution of substrate specificities in the P-type ATPase superfamily, *J. Mol. Evol. 46*, 84−101.
3. Nucifora, G., Chu, L., Misra, T. K., and Silver, S. (1989) Cadmium resistance from *Staphylococcus aureus* plasmid pI258 cadA gene results from a cadmium-efflux ATPase, *Proc. Natl. Acad. U.S.A. 86*, 3544−3548.
4. Mercer, J. F., Livingston, J., Hall, B., Paynter, J. A., Begy, C., Chandrasekharappa, S., Lockhart, P., Grimes, A., Bhave, M., Siemieniak, D., and Glover, T. W. (1993) Isolation of a partial candidate gene for Menkes disease by positional cloning, *Nat. Genet. 3*, 20−25.
5. Vulpe, C., Levinson, B., Whitney, S., Packman, S., and Gitschier, J. (1993) Isolation of a candidate gene for Menkes disease and evidence that it encodes a copper-transporting ATPase, *Nat. Genet. 3*, 7−13.
6. Bull, P. C., Thomas, G. R., Rommens, J. M., Forbes, J. R., and Cox, D. W. (1993) The Wilson disease gene is a putative copper transporting P-type ATPase similar to the Menkes gene, *Nat. Genet. 5*, 327−337.
7. Odermatt, A., Suter, H., Krapf, R., and Solioz, M. (1993) Primary structures of two P-type ATPases involved in copper resistance in *Enterococcus hirae*, *J. Biol. Chem. 268*, 12775−12779.
8. Rensing, C., Mitra, B., and Rosen, B. P. (1997) The *znt*A gene of *Escherichia coli* encodes a Zn^{2+}-translocating P-type ATPase, *Proc. Natl. Acad. Sci. U.S.A. 94*, 14326−14331.
9. Rensing, C., Sun, Y., Mitra, B., and Rosen, B. P. (1998) Pb^{2+}-translocating P-type ATPases, *J. Biol. Chem. 273*, 32614−32617.
10. Rutherford, J. C., Cavet, J. S., and Robinson, N. (1999) Cobalt-dependent transcriptional switching by a dual-effector MerR-like protein regulates a cobalt-exporting variant CPx-type ATPase, *J. Biol. Chem. 274*, 25827−25832.
11. Gupta, A., Matsui, K., Lo, J. F., and Silver, S. (1999) Molecular basis for resistance to silver cations in *Salmonella*, *Nat. Med. 5*, 183−188.
12. Rensing, C., Fan, B., Sharma, R., Mitra, B., and Rosen, B. P. (2000) CopA: an *Escherichia coli* Cu(I)-translocating P-type ATPase, *Proc. Natl. Acad. Sci. U.S.A. 97*, 652−656.
13. Mandal, A. K., Cheung, W. D., and Arguello, J. M. (2002) Characterization of a thermophilic P-type Ag^{+}/Cu^{+}-ATPase from the extremophile *Archaeoglobus fulgidus*, *J. Biol. Chem. 277*, 7201−7208.
14. Mana-Capelli, S., Mandal, A. K. and Arguello, J. M. (2003) *Archaeoglobus fulgidus* CopB is a thermophilic Cu^{2+}-ATPase: functional role of its histidine-rich-N-terminal metal binding domain, *J. Biol. Chem. 278*, 40534−40541.
15. Lutsenko, S., Petrukhin, K., Cooper, M. J., Gilliam, C. T., and Kaplan, J. H. (1997) N-terminal domains of human copper-transporting adenosine triphosphatases (the Wilson's and Menkes disease proteins) bind copper selectively in vivo and in vitro with stoichiometry of one copper per metal-binding repeat, *J. Biol. Chem. 272*, 18939−18944.
16. DiDonato, M., Narindrasorasak, S., Forbes, J. R., Cox, D. W., and Sarkar, B. (1997) Expression, purification, and metal binding properties of the N-terminal domain from the Wilson disease putative copper-transporting ATPase (ATP7B), *J. Biol. Chem. 272*, 33279−33282.
17. Cobine, P. A., George, G. N., Winzor, D. J., Harrison, M. D., Mogahaddas, S., and Dameron, C. T. (2000) Stoichiometry of complex formation between Copper(I) and the N-terminal domain of the Menkes protein, *Biochemistry 39*, 6857−6863.
18. Ralle, M., Lutsenko, S., and Blackburn, N. J. (2003) The Menkes disease protein binds copper via novel 2-coordinate Cu^{+}-cysteinates in the N-terminal domain, *J. Biol. Chem. 278*, 23163−23170.
19. Liu, J., Stemmler, A. J., Fatima, J., and Mitra, B. (2005) Metal-binding characteristics of the amino-terminal domain of ZntA: Binding of lead is different compared to cadmium and zinc, *Biochemistry 44*, 5159−5167.
20. Liu, J., Dutta, S. J., Stemmler, A. J., and Mitra, B. (2006) Metal-binding affinity of the transmembrane site in ZntA: implications for metal selectivity, *Biochemistry 45*, 763−772.
21. Arguello, J. M. (2003) Identification of ion-selectivity determinants in heavy-metal transport P1B-type ATPases, *J. Membr. Biol. 195*, 93−108.
22. Banci, L., Bertini, I., Ciofi-Baffoni, S., Finney, L. A., Outten, C. E., and O'Halloran, T. V. (2002) A new zinc-protein coordination site in intracellular metal trafficking: solution structure of the Apo and Zn(II) forms of ZntA(46−118.), *J. Mol. Biol. 323*, 883−897.

23. Banci, L., Bertini, I., Ciofi-Baffoni, S., Su, X. C., Miras, R., Bal, N., Mintz, E., Catty, P., Shokes, J. E., and Scott, R. A. (2006) Structural basis for metal binding specificity: the N-terminal cadmium binding domain of the P1-type ATPase CadA, *J Mol. Biol. 356*, 638−650.
24. Sharma, R., Rensing, C., Rosen, B. P., and Mitra, B. (2000) The ATP hydrolytic activity of purified ZntA, a $Pb^{2+}/Cd^{2+}/Zn^{2+}$-translocating ATPase from *Escherichia coli*, *J. Biol. Chem. 275*, 3873−3878.
25. Fan, B., and Rosen, B. P. (2002) Biochemical characterization of CopA, the *Escherichia coli* Cu(I)-translocating P-type ATPase, *J. Biol. Chem. 277*, 46987−46992.
26. Mandal, A. K., and Arguello, J. M. (2003) Functional roles of metal binding domains of the *Archaeoglobus fulgidus* Cu(+)-ATPase CopA, *Biochemistry 42*, 11040−11047.
27. Bal, N., Wu, C. C., Catty, P., Guillain, F., and Mintz, E. (2003) Cd^{2+} and the N-terminal metal-binding domain protect the putative membranous CPC motif of the Cd^{2+}-ATPase of *Listeria monocytogenes*, *Biochem. J. 369*, 681−685.
28. Wu, C. C., Gardarin, A., Martel, A., Mintz, E., Guillain, F., and Catty, P. (2006) The cadmium transport sites of CadA, the Cd^{2+-}ATPase from *Listeria monocytogenes*, *J. Biol. Chem. 281*, 29533−29541.
29. Dutta, S. J., Liu, J., Hou, Z., and Mitra, B. (2006) Conserved Asp714 in transmembrane segment 8 of the ZntA subgroup of P_{1B}-type ATPases is a metal-binding residue, *Biochemistry 45*, 5923−5931.
30. Riddles, P. W., Blakeley, R. L., and Zerner, B. (1979) Ellman's reagent: 5,5′-dithiobis(2-nitrobenzoic acid)−a reexamination, *Anal. Biochem. 94*, 75−81.
31. Mitra, B., and Sharma, R. (2001) The cysteine-rich amino-terminal domain of ZntA, a Pb(II)/Cd(II)/Zn(II)-translocating ATPase from *Escherichia coli*, is not essential for its function, *Biochemistry 40*, 7694−7699.
32. Hou, Z., and Mitra, B. (2003) Characterization of the metal specificity of ZntA from *Escherichia coli* using the acylphosphate intermediate, *J. Biol. Chem. 278*, 28455−28461.
33. Kuzmic, P. (1996) Program DYNAFIT for the analysis of enzyme kinetic data: application to HIV proteinase, *Anal. Biochem. 237*, 260−273.
34. Sigel, H. (1987) Isomeric equilibria in complexes of adenosine 5′-triphosphate with divalent metal ions. Solution structures of M(ATP)2- complexes, *Eur. J. Biochem. 165*, 65−72.
35. Simons, T. J. (1993) Measurement of free Zn^{2+} ion concentration with the fluorescent probe mag-fura-2 (furaptra), *J. Biochem. Biophys. Methods 27*, 25−37.
36. Martell, A. E., and Smith, R. M. (1974) *Critical Stability Constants Vol.1: Amino Acids*, Vol II, Plenum Press, New York, Florida, 206−208.
37. Hou, Z-J., Narindrasorasak, S., Bhushan, B., Sarkar, B., and Mitra, B. (2001) Functional analysis of chimeric proteins of the Wilson Cu(I)-transporting ATPase (ATP7B) and ZntA, a Pb(II)/Zn(II)/Cd(II)-translocating ATPase from *Escherichia coli*, *J. Biol. Chem. 276*, 40858−40863.
38. Dutta, S. J., Liu, J., and Mitra, B. (2005) Kinetic analysis of metal binding to the amino-terminal domain of ZntA by monitoring metal-thiolate charge-transfer complexes, *Biochemistry 44*, 14268−14274.
39. Magyar, J. S., Weng, T. C., Stern, C. M., Dye, D. F., Rous, B. W., Payne, J. C., Bridgewater, B. M., Mijovilovich, A., Parkin, G., Zaleski, J. M., Penner-Hahn, J. E., and Godwin, H. A. (2005) Reexamination of lead(II) coordination preferences in sulfur-rich sites: implications for a critical mechanism of lead poisoning, *J. Am. Chem. Soc. 127*, 9495−9505.
40. Wang, Y., Hemmingsen, L., and Giedroc, D. P. (2005) Structural and functional characterization of *Mycobacterium tuberculosis* CmtR, a PbII/CdII-sensing SmtB/ArsR metalloregulatory repressor, *Biochemistry 44*, 8976−8988.
41. Lowe, J., Vieyra, A., Catty, P., Guillain, F., Mintz, E., and Cuillel, M. (2004) A mutational study in the transmembrane domain of Ccc2p, the yeast Cu(I)-ATPase, shows different roles for each Cys-Pro-Cys cysteine. *J. Biol. Chem. 279*, 25986−25994.

BI0616394